

Revisiting the Closed Loop Response of PWM Converters Controlled by Voltage Feedback

Mor Mordechai Peretz and Sam Ben-Yaakov
Power Electronics Laboratory
Department of Electrical and Computer Engineering
Ben-Gurion University of the Negev
P.O. Box 653, Beer-Sheva 84105, ISRAEL.
Phone: +972-8-646-1561; Fax: +972-8-647-2949;
Emails: morp@ee.bgu.ac.il, sby@ee.bgu.ac.il ; Website: www.ee.bgu.ac.il/~pel

Abstract- The closed loop response of voltage feedback converters was re-examined theoretically and tested by simulations and experiments.

It was found that the classical second order representation of the closed loop response of a PID controlled system is incomplete due to the contribution of previously neglected factors, such as a closed loop zero and low loop gain, to the real response. Mathematical expressions of the closed loop responses that take into account these added factors were derived and the time domain attributes (rise time and overshoot) were extracted.

The method is exemplified by an experimental Buck and Boost converters that were operated in voltage mode control using a lag-lead phase compensation network.

I. INTRODUCTION

With the rising interest in digital power management, the use of voltage feedback control in PWM DC-DC converters is regaining popularity since it is considered a cost-effective and feasible solution in present-day digital technology. The reason for this popularity is primarily the difficulty of implementing a fast digitally controlled inner loop, such as required in peak current mode control.

The voltage feedback scheme often applies lag-lead network (PID structure compensator) to regulate the output voltage and set the desired dynamic response. The traditional design of such feedback structure specifies that the phase margins of the system be around 45° . The corresponding dynamic response (rise time and overshoot) can then be estimated by the known relationships of a second order system [1-3]. However, in practical systems it is often observed that the influence of poles and zeros near the crossover frequency can not be overlooked. In particular, as discussed in this paper, the closed loop response of PWM converters with voltage feedback can not be described, in the general case, by a second order template. Consequently, the classical relationship between the phase margin, and rise time and overshoot [1-3] are not valid in such cases. For example, consider a typical PWM DC-DC converter of a second order that is controlled by a conventional lag-lead compensator designed to close the loop in the region of the -40dB/dec slope of the plant with a phase margin of 60° . According to the conventional approach, the closed loop response would be assumed to be of a second order and will have a relatively small overshoot (Fig. 1). In reality, however, the actual transient response of such a

system is substantially different from the assumed second order response (Fig. 1), in terms of both the rise time and the overshoot. Two reasons can be identified as causing a deviation from the ideal second order response. One is the presence of a zero in the closed loop response [1-3]. The second reason is a low loopgain over an extended portion of the useful frequency range. These deviations have been mentioned in earlier publications [1-3] and handled by trial and error procedure. No rigorous treatment of these issues and their influence of the closed loop response dynamics have been conducted hitherto. The objective of this work was to explore these cases and their influence on the closed loop response and develop a methodology for quantifying the system transient attributes.

The results of this investigation could assist in the design of analog and digital voltage feedback loops in PWM converters when the design goal is to obtain a fast dynamic response, and could potentially eliminate the need for a trial and error procedure.

II. DERIVATION OF CLOSED-LOOP RESPONSES: APPROXIMATION METHOD

A typical single control loop system can be generally described by the block diagram of Fig. 2. It comprises the system's plant $A(s)$, and the compensator $B(s)$. Without losing generality, the system is normalized here to a unity feedback ratio (in a practical system this term would be a constant: the voltage divider ratio). The error signal, S_e , is generated by comparing the sensed output to the desired reference input, S_{ref} .

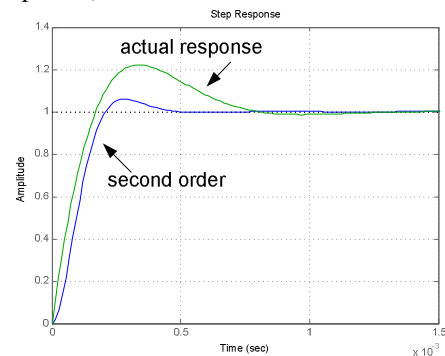


Figure 1. Step response of system in closed loop. Comparison of a second order model to the time domain simulation response.

The overall closed-loop Transfer Function (TF) of the system (Fig. 2) will be:

$$A_{CL}(s) = \frac{A(s)B(s)}{1 + A(s)B(s)} \quad (1)$$

It implies that as long as the magnitude of the product $A(s)B(s)$ is sufficiently larger than 1, the output signal will follow reference with no delay or attenuation, however, when the loop gain $A(s)B(s)$ approaches unity, the response of the system will be determined by the interaction of $A(s)$ and $B(s)$.

A voltage feedback loop typically includes a power stage of a second order ($A(s)$, Fig. 3):

$$A(s) = \frac{k_p \left(\frac{s}{\omega_{pz}} + 1 \right)}{s^2 / \omega_{pn}^2 + s / \omega_{pn} Q_p + 1} \quad (2)$$

where k_p is the plant's gain factor, ω_{pn} and Q_p are the plant's natural frequency and quality factor respectively, and ω_{pz} is the frequency of the high frequency zero.

The general description of the compensator will be of a lag-lead type ($B(s)$, Fig. 3):

$$B(s) = \frac{\left(\frac{s}{\omega_{c2}} + 1 \right) \left(\frac{s}{\omega_{c3}} + 1 \right)}{s / \omega_{c1}} \quad (3)$$

where ω_{c1} , ω_{c2} and ω_{c3} are the pole and zeros placements of $B(s)$. It should be noted that the complete response of $B(s)$ includes another pole at very high frequency (Fig. 3) and hence its influence is small, and thus is neglected here.

It should also be noted that due to the non-linear nature of PWM power converters, the transfer functions described in (2) and (3) and those that are developed further below, refer to the small-signal response of the system that is linearized around specified operating conditions. That is, for a specific input voltage, output voltage and load conditions. For every bias settings, the parameters K_p and Q_p may change such that $A(s)$ will describe the plant response for the specified bias point.

To determine the response of the system in closed loop, it is essential to know where and how the loopgain TF crosses 0dB, or more accurately, assuming that the product $A(s)B(s)$ is larger than 1 at frequencies far from 0dB point, the behavior of the loopgain at frequencies in the vicinity of the crossover frequency will determine the response of the system in closed loop [4].

As we apply this concept, we distinguish between three possible cases that can be encountered when using the PID type compensator: the plant has a constant gain (Fig. 4), has a -40dB/dec slope (Fig. 7) or has a -20dB/dec slope (Fig. 8).

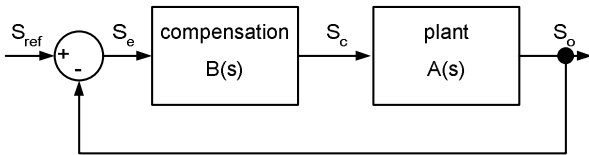


Figure 2. Single-loop control scheme, simplified block diagram.

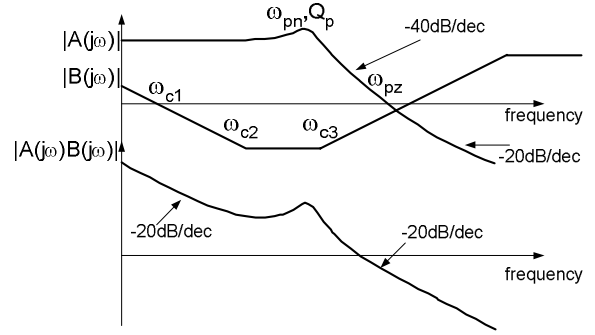


Figure 3. General description of retransfer functions. Plant $A(j\omega)$, compensator $B(j\omega)$ and loopgain. $A(j\omega)B(j\omega)$

In this study we denote the cases by their location with respect to the plant's double pole location (ω_{pn}).

In the first case (Fig. 4), a PI type compensator is used to set the loopgain 0dB point at the region of the plant constant gain, below ω_{pn} . The plant and the compensator in the vicinity of the crossover can be approximated to:

$$A(s) = \frac{1}{\left(\frac{s}{\omega_{bl}} + 1 \right)^2} \quad (4) \quad ; \quad B(s) = \frac{k \left(\frac{s}{\omega_{bl}} + 1 \right)}{s / \omega_{crs}} \quad (5)$$

where ω_{crs} and ω_{bl} are the poles and zeros frequencies of Fig. 5 and $k = \sqrt{1 + (\omega_{crs} / \omega_{bl})^2}$ is the controller gain calculated to match the crossover frequency of ω_{crs} .

$$A(s)B(s) = \frac{k}{s / \omega_{crs} \left(\frac{s}{\omega_{bl}} + 1 \right)} \quad (6)$$

The derived loopgain (Fig. 5) has two poles at ω_{crs} and ω_{bl} , it reaches 0dB at ω_{crs} with a Rate-of-Closer (ROC) between -20 dB/dec and -40dB/dec depending on the vicinity of these frequencies.

The phase margin of this case can be obtained by replacing 's' by 'jω' in (6), equating it to 1 and solving for 'ω',

$$\varphi_m = \text{tg}^{-1} \left(\frac{\omega_{bl}}{\omega_{crs}} \right) \quad (7)$$

For the private case in which ω_{crs} and ω_{bl} are relatively far apart, in the range of one decade or more, the phase margin will be around 90° and the closed-loop TF will follow the simple form of a low-pass with two real poles:

$$A_{CL_bl}(s) = \frac{k}{\left(\frac{s}{\omega_{bl}} + 1 \right) \left(\frac{s}{\omega_{crs}} + 1 \right)} \quad (8)$$

In the general case, the closed-loop TF (Fig. 6) will be of a second order, that is

$$A_{CL}(s) = \frac{1}{s^2 / k \omega_{bl} \omega_{crs} + s / \omega_{crs} + 1} \quad (9)$$

Eq. (9) is the typical, well known, form of response that is assumed in conventional feedback design [3]. However, there are cases in which (9) is insufficient to describe the response and additional frequency factors are needed. These situations, which are the object of this study, can be

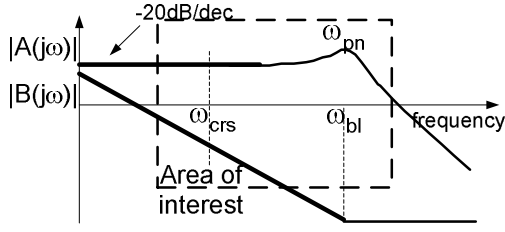


Figure 4. Plant and compensator TFs. Crossover below ω_{pn} in the region of constant gain of the plant.

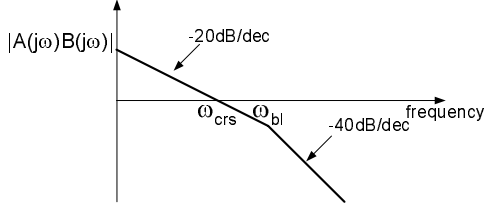


Figure 5. Loopgain transfer function. Crossover below ω_{pn} . Corresponding to Fig. 4.

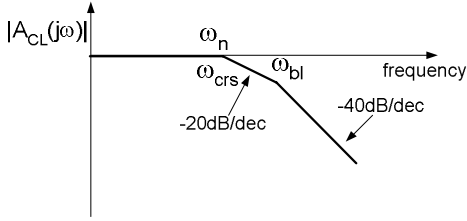


Figure 6. Closed-loop transfer function Crossover below ω_{pn} . Corresponding to Fig. 5.

viewed in the other two cases of Fig. 7 and Fig. 8, where a PID compensator is applied to set the crossover frequency in region higher than ω_{pn} . For the case depicted in Fig. 7, the relevant TFs are:

$$A(s) = \frac{1}{s^2 / \omega_{abv}^2} \quad (10) \quad ; \quad B(s) = \frac{\omega_{crs}}{k \omega_{abv}} \left(\frac{s}{\omega_{abv}} + 1 \right) \quad (11)$$

and for the case of Fig. 8

$$A(s) = \frac{1}{s / \omega_{abv}} \quad (12) \quad ; \quad B(s) = \frac{1}{k} \frac{s / \omega_{crs}}{s / \omega_{abv} + 1} \quad (13)$$

where the controller gain $k = 1 / \sqrt{1 + (\omega_{abv} / \omega_{crs})^2}$ is now adjusted to match the crossover frequency of ω_{crs} which is higher than ω_{pn} .

The loopgain TF (for both cases) in the vicinity of the crossover (Fig. 9) will now be:

$$A(s)B(s) = \frac{k \left(\frac{s}{\omega_{abv}} + 1 \right)}{s^2 / \omega_{abv} \omega_{crs}} \quad (14)$$

By following the same concept as in (7), the phase margin for this case is found to be:

$$\varphi_m = \text{tg}^{-1} \left(\frac{\omega_{crs}}{\omega_{abv}} \right) \quad (15)$$

The derived loopgain of these cases has a double pole at $\omega_{abv} \omega_{crs}$ and zero at ω_{abv} , it reaches 0dB at ω_{crs} with a ROC of approximately -40 dB/dec to -20dB/dec depending on the

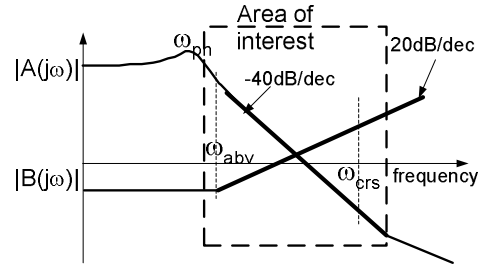


Figure 7. Plant and compensator TFs. Crossover above ω_{pn} in the region of -40dB/dec of the plant.

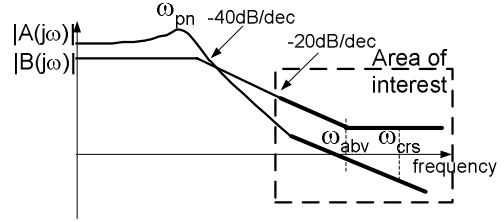


Figure 8. Plant and compensator TFs. Crossover above ω_{pn} in the region of -20dB/dec of the plant.

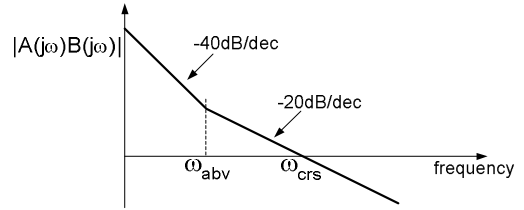


Figure 9. Loopgain transfer function. Crossover above ω_{pn} . Corresponding to Figs. 7 and 8.

location of these frequencies. In the private case that the phase margin is 90° , that is, ω_{abv} is in the range of a decade or more than ω_{crs} , the system in closed-loop can be simplified to the form:

$$A_{CL_abv}(s) = \frac{\left(\frac{s}{\omega_{abv}} + 1 \right)}{k \left(\frac{s}{\omega_{abv}} + 1 \right) \left(\frac{s}{\omega_{crs}} + 1 \right)} \quad (16)$$

For the general case, the closed loop TF will be (Fig. 10):

$$A_{CL_abv}(s) = \frac{\frac{s}{\omega_{abv}} + 1}{s^2 / k \omega_{abv} \omega_{crs} + \frac{s}{\omega_{abv}} + 1} \quad (17)$$

By examination of (7) and (17), one can obtain a unified closed loop TF for all three cases as:

$$A_{CL}(s) = \frac{\frac{s}{\omega_z} + 1}{s^2 / k \omega_1 \omega_2 + \frac{s}{\omega_1} + 1} \quad (18)$$

where (for the case of Fig. 4): $\omega_z = \infty$; $\omega_1 = \omega_{crs}$; $\omega_2 = \omega_{bl}$. And for the other two cases (Figs. 7 and 8): $\omega_z = \omega_{abv}$; $\omega_1 = \omega_{abv}$; $\omega_2 = \omega_{crs}$.

The generic expression of the phase margin will thus be:

$$\varphi_m = \text{tg}^{-1} \left(\frac{\omega_2}{\omega_1} \right) \quad (19)$$

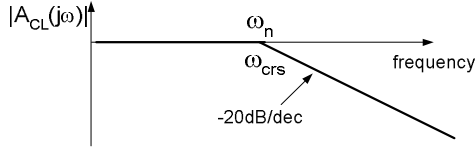


Figure 10. Closed-loop transfer function. Crossover above ω_{pn} . Corresponding to Fig. 9.

By comparing the characteristic equation of (18) to a general second order template [1, 3], the unified expressions of the natural frequency ω_n and the quality factor Q are found to be:

$$\omega_n = \sqrt{k\omega_1\omega_2} \quad (20)$$

$$Q = \sqrt{\frac{k\omega_1}{\omega_2}} \quad (21)$$

Combining (20) and (21) and after some manipulations, the quality factor in terms of the phase margins is found to be:

$$Q = \frac{\sqrt{\cos \varphi_m}}{\sin \varphi_m} \quad (22)$$

By observing the derived loop gains of both cases, it can be seen that they have a similar ROC of -20dB/dec, and their closed loop has a similar characteristic equation. This may lead an erroneous conclusion that they will have a similar dynamic response. However, comparison of the full term TFs reveals some distinctive differences between the two closed loop situations. Notwithstanding the fact that both of the loop gains cross 0dB with ROC of -20dB/dec, the loop gain in (6) has a pole after 0dB cross over whereas (14) is descending at a rate of -40dB/dec and the zero near the crossover reverses the ROC to -0dB/dec. This implies that the system of (14) will have higher loop gain throughout the area prior to the crossover frequency. Detailed analysis of this effect is carried out in the following section.

III. EFFECTS OF CLOSED-LOOP ZERO ON THE DYNAMIC RESPONSE

As pointed out in the previous chapter, the key to determining the response of a system in closed loop depends on the behavior of the loop gain around the crossover frequency. As seen in (17) (Fig. 10), the closed-loop response will no longer be of a simple second order form due to the influence of a closed-loop zero. This situation, in fact, is quite common in power electronics feedback design, where a power stage is regulated in voltage-mode control using a lag-lead network [5-7]. By applying the approximation method described in the previous chapter, the dynamic response of the closed loop system in these cases was derived, taking into account effect of the zero.

Consider the example of Fig. 3 which corresponds the second order plant of (2), controlled by a lag-lead network of (3). It is assumed that the compensator is designed to set the crossover frequency in the region of

$$\omega > \omega_{pn} \quad (23)$$

The relevant TFs of (2) and (3) can be approximated by:

$$A(s) = \frac{k_p}{s^2 / \omega_{pn}^2 + s / \omega_{pn} Q_p} \quad (24)$$

$$B(s) = \frac{\omega_{c1}}{\omega_{c2}} \left(\frac{s}{\omega_{c3}} + 1 \right) \quad (25)$$

The closed-loop TF as a function of the system parameters can then be written as

$$A_{CL}(s) = \frac{s / \omega_{c3} + 1}{s^2 \frac{\omega_{c2}}{k_p \omega_{c1} \omega_{pn}^2} + s \left(\frac{\omega_{c2}}{k_p \omega_{c1} \omega_{pn} Q_p} + \frac{1}{\omega_{c3}} \right) + 1} \quad (26)$$

The closed loop natural frequency ω_n and the quality factor Q can be identified as

$$\omega_n = \omega_{pn} \sqrt{\frac{k_p \omega_{c1}}{\omega_{c2}}} \quad (27)$$

$$Q = \frac{\sqrt{k_p \omega_{c1} \omega_{c2} \omega_{c3} Q_p}}{\omega_{c2} \omega_{c3} + k_p \omega_{c1} \omega_{pn} Q_p} \quad (28)$$

To obtain the time-domain response, first (26) is rewritten as the sum of two Laplace functions. After some manipulations one obtains

$$A_{CL}(s) = \frac{k_1(s+a)}{(s+a)^2 + b^2} + \frac{k_2 b}{(s+a)^2 + b^2} \quad (29)$$

where $a = \frac{\omega_n}{2Q}$; $b = \omega_n \sqrt{1 - \frac{1}{4Q^2}}$;

$$k_1 = \frac{\omega_n^2}{\omega_{c3}} \quad ; \quad k_2 = \omega_n \left(1 - \frac{\omega_n}{2Q \omega_{c3}} \right) / \sqrt{1 - \frac{1}{4Q^2}}$$

Then, dividing (29) by the Laplace operator 's' and taking the inverse transform will yield the closed-loop step response. After some manipulations one obtains

$$y_{\text{unit_step}} = 1 - \sqrt{\frac{k_1^2 + k_2^2}{a^2 + b^2}} e^{-at} \cos \left(bt + \text{tg}^{-1} \left(\frac{b}{a} \right) + \text{tg}^{-1} \left(\frac{k_2}{k_1} \right) \right) \quad (30)$$

Equation (30) is the transient step response extraction of the small-signal closed-loop TF (26) and thus describes the response of the system around the operation point for which (26) applies. The unity step is used here as a scaling factor that represents the transition between one operating conditions (some nominal value) to another in the range that is still considered small-signal.

The generic transient response of (30) is depicted in Fig. 11. Rise time is defined in this study as the duration between the starting point of the step perturbation until the step response of the system reaches the new nominal value. This was defined in this way because (a) it can be linearly solved, (b) it found to provide a physical interpretation of the closed loop dynamics, and (c) it is a good approximation to the formal definition. The overshoot was defined in the classical way: as the ratio of the maximum positive deviation from the nominal value.

To obtain a generalized view of the response we normalize the factors ω_{c3} and ω_{pn} (Fig. 3) to the natural frequency ω_n by

setting: $m = \omega_{c3}/\omega_n$, and $n = \omega_{pn}/\omega_n$, the normalized form of the closed-loop quality factor takes the form:

$$Q = \frac{1}{\frac{n}{Q_p} + \frac{1}{m}} \quad (31)$$

Along with the specification of the plant's quality factor (Q_p), the parameters 'm' and 'n' provide the full physical information needed for the design of a feedback loop in terms of the behavior of the plant, desired bandwidth and the closed loop zero location.

Equating (30) to unity and solving for the parameter 't' will yield the rise time of the step response, as defined in this study (normalization was obtained by multiplying the result by ω_n)

$$\omega_n t_r = \frac{2Q}{\sqrt{4Q^2 - 1}} \left[\text{tg}^{-1} \left(\frac{1}{\sqrt{4Q^2 - 1}} \right) - \text{tg}^{-1} \left(-\frac{2Qm - 1}{\sqrt{4Q^2 - 1}} \right) \right] \quad (32)$$

Taking the derivative of (30), equating to zero and solving for the parameter 't' will yield the time instance at which (30) reaches the maximum value

$$t_p = \frac{1}{b} \text{tg}^{-1} \left(-\frac{k_1}{k_2} \right) \quad (33)$$

It should be noted that the formal trigonometric solution produces a periodic result for all possible maxima points, however, the most significant overshoot of (30), that is, the absolute maximum of the function, will occur at the first time interval which is the object of the derivation. Inserting 't_p' into (30) and after some manipulations, the normalized overshoot is found to be:

$$M_p = \left(1 - \frac{1}{2Qm} \right) \exp \left(-\text{tg}^{-1} \left[-\frac{\sqrt{1 - \frac{1}{4Q^2}}}{m \left(1 - \frac{1}{2Qm} \right)} \right] / \sqrt{4Q^2 - 1} \right) \quad (34)$$

Figs. 12 to 15 show the normalized curves of (32) and (34) as a function of the ratios 'm' and 'n' for two cases of the plant quality factor Q_p . The plots reveal that the rise time increases with the increase of 'm' and 'n'. The overshoot is found to be linearly proportional to 'm', but inversely proportional with 'n'. The value of Q_p sets the slope. It should be noted that the upper limit for the parameter 'n' is 1 to assure that the crossover frequency is higher than ω_{pn} as set in (23).

The physical interpretation of these results is as follows: as we set the zero location of ω_{c3} to higher frequencies above ω_n (increase of 'm'), the loopgain will be forced to cross 0dB at higher ROC which will cause the system to be less damped, will cause a faster rise time, a higher overshoot and may even

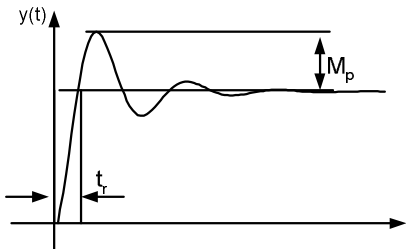


Figure 11. Typical step response of system with overshoot and definitions of dynamic parameters: rise time t_r and overshoot M_p.

threat the system's stability. The influence of changes 'n', is slightly different. For a constant 'm', as we push the crossover frequency toward ω_{pn} we reduce the system gain and bandwidth. This may end up in poorer dynamic response in the form of longer transients.

IV. EFFECTS OF LOW LOOPGAIN BELOW THE CROSSOVER FREQUENCY

Up to this point in this study, the concept of approximating the closed loop response by the local behavior of the loopgain in the vicinity of the crossover frequency was justified under the assumption that the effects of other poles or zeros that are far from this point is negligibly small due to high loopgain. There are cases however [7, 8], that this does not apply and the complete response of A(s)B(s) is needed to determined the closed loop response. Fig. 16 exemplify such a situation, the loopgain is of low value in an extended frequency region below the crossover frequency. To tackle this problem we can separate the loopgain into two sections based on the high and low frequency contributions of the compensator (Fig. 17): The effect of the lead (high frequency) component (which was derived in the previous section) and the effect of the lag (low frequency) component on the closed loop. Then, the step response of the system (Fig. 18) is a result of the lag (low frequency) response (Fig. 19) plus the high frequency contribution that was discussed in the previous section.

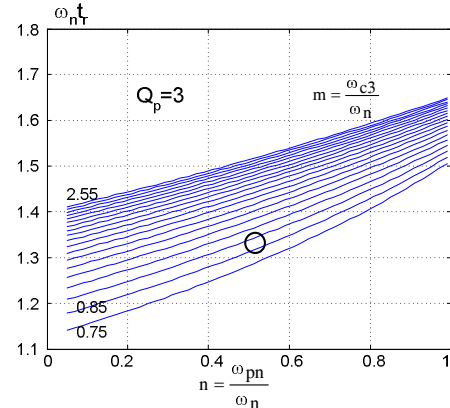


Figure 12. Normalized rise time as a function of the normalized frequency deviations 'm' and 'n', $Q_p=3$. 'O' - experimental point

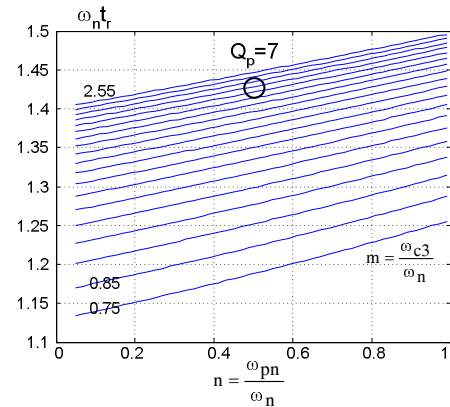


Figure 13. Normalized rise time as a function of the normalized frequency deviations 'm' and 'n', $Q_p=7$. 'O' - experimental point

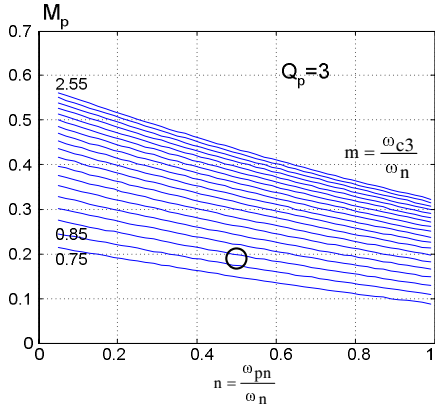


Figure 14. Normalized overshoot as a function of the normalized frequency deviations 'm' and 'n', $Q_p=3$. 'O' – experimental point

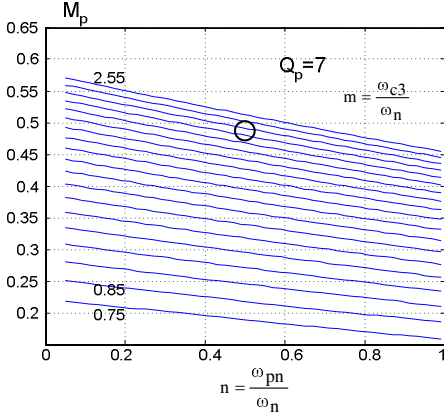


Figure 15. Normalized overshoot as a function of the normalized frequency deviations 'm' and 'n', $Q_p=7$. 'O' – experimental point

The frequency region of interest is:

$$\omega < \omega_{pn} \quad (35)$$

The relevant responses for plant $A(s)$ and the compensator $B(s)$ would be:

$$A(s) = k_p \quad (36) \quad ; \quad B(s) = \frac{\left(\frac{s}{\omega_{c2}} + 1\right)}{\frac{s}{\omega_{c1}}} \quad (37)$$

The addition to the closed loop due to the low loopgain is then found to be:

$$A_{CL_lag}(s) = \frac{\frac{s}{\omega_{c2}} + 1}{s \left/ \left(\frac{k_p \omega_{c1} \omega_{c2}}{\omega_{c2} + k \omega_{c1}} \right) + 1 \right.} \quad (38)$$

or in the time domain:

$$y_{unit_step_lag}(t) = 1 - \frac{1}{1 + \frac{k_p \omega_{c1}}{\omega_{c2}}} e^{-\omega_{c2} t} \quad (39)$$

From (38) and (39) it can be observed that the effect of this part on the closed loop response is largely dependent on $k_p \omega_{c1} / \omega_{c2}$ that is, on the loopgain magnitude at mid frequencies. As this gain increases, the pole and zero of (38) become closer and cancel each other. Fig. 19 shows curves of (39) for different gains. At high gains, the unit step passes thru with no

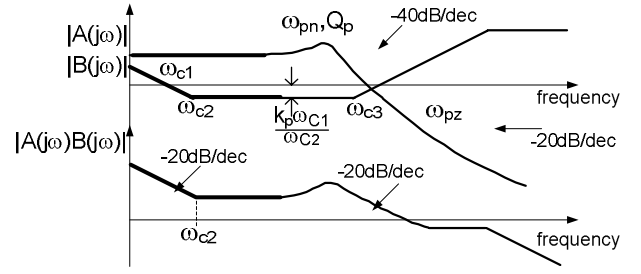


Figure 16. Plant, compensator and loopgain TFs. System's gain is low.

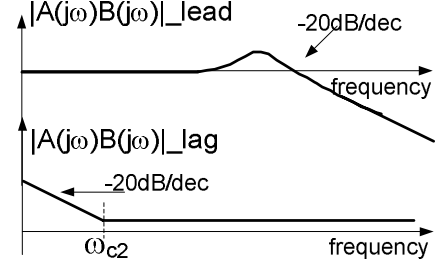


Figure 17. Decomposition of the loopgain into a lag and lead parts of the low gain situation.

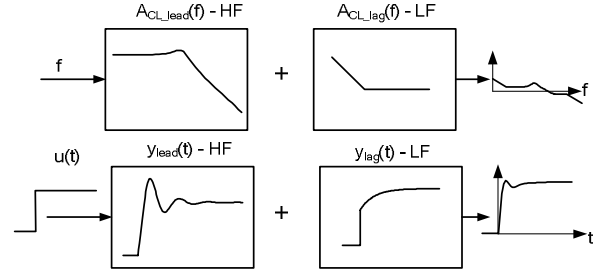


Figure 18. Contribution of the lag part and lead part to the system closed-loop response. Upper path. Frequency domain. Lower path: Time domain.

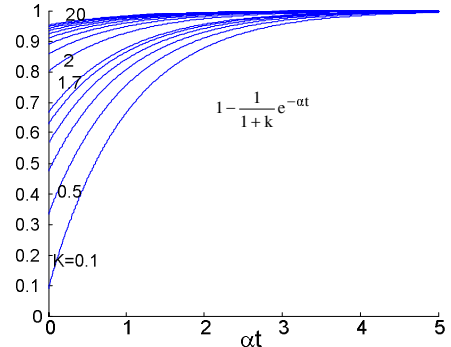


Fig. 19. Contribution of the lag compensation to the step response of the system in closed loop.

delay or attenuation, however, as the gain decreases, the system is more prone to the effect of the low frequency pole ω_{c2} that results in longer settling periods.

V. SIMULATION AND EXPERIMENTAL RESULTS

The proposed analysis was verified by comparison of the analytical derivations to a PSPICE average simulation and then was crosschecked against experimental measurements. The experimental part included Buck and Boost power stages that were controlled by lag-lead network around a UC3843 (Texas Instruments) PWM controller that was operated in voltage-mode configuration.

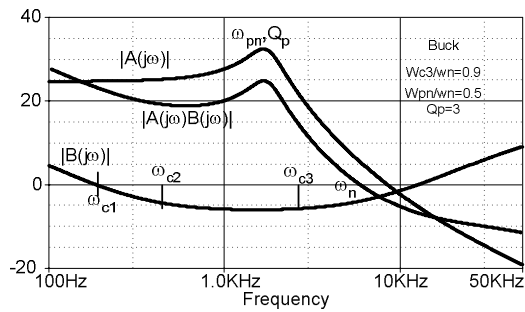


Figure 20. Simulation of experimental Buck converter system and the relevant break points locations.

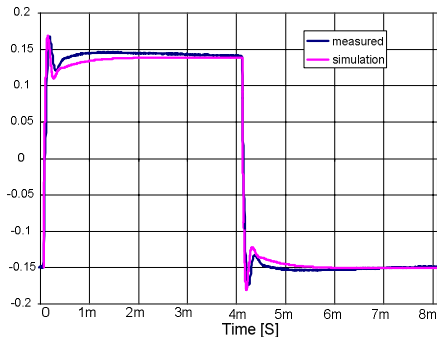


Figure 21. Measured and simulated step response of a Buck converter operated in closed loop.

The effect of the closed-loop zero was obtained by subjecting the closed-loop system to a step in the reference and measuring the output response. A Buck type converter was controlled by a lag-lead network. The relevant TFs are given in Fig. 20, the frequency ratios were $m=0.9$, $n=0.5$, $Q_p=3$ and loopgain crossover frequency at 3.3KHz. The step response (measured and simulation, Fig. 21) attributes were found to be $t_r=70\mu S$ and $M_p=15\%$. The theoretical values are circled in Figs. 12 and 14. As another example, a Boost type converter was controlled by a lag-lead network. The relevant TFs are given in Fig. 22, the frequency ratios were $m=2.5$, $n=0.52$, $Q_p=7$ and loopgain crossover frequency at 1.6KHz. The step response (measured and simulated, Fig. 23) attributes were found to be $t_r=70\mu S$ and $M_p=15\%$. The theoretical values are circled in Figs. 13 and 15.

VI. CONCLUSIONS

This study quantifies the closed loop dynamic response of voltage feedback converters. The analytical methodology, used here was based on reducing the order of the full term loopgain function at the frequencies where the system gain is high and then extracting the closed loop response from the approximated function. The analytical results were found to match the simulation and the experimental results.

The analysis revealed that the closed loop response depend not only on the crossover frequency and the phase margin but also on where the crossover frequency is located with respect to the plant behavior. It was found that a system designed with bandwidth above the plant's double pole ω_{pn} will introduce a closed loop zero term and thus will have a lead effect on the system that results in faster response and higher overshoot.

The analytical results for the rise time and overshoot for bandwidth settings above the open loop resonant frequency, indicates that when the zero location is moved to be at higher frequencies than the crossover frequency, the phase margin will decrease and the system will be less damped.

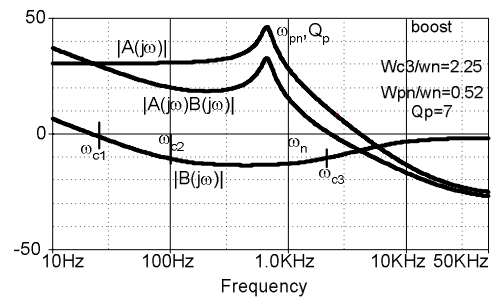


Fig. 22. Simulation of experimental Boost converter system and the relevant frequency locations.

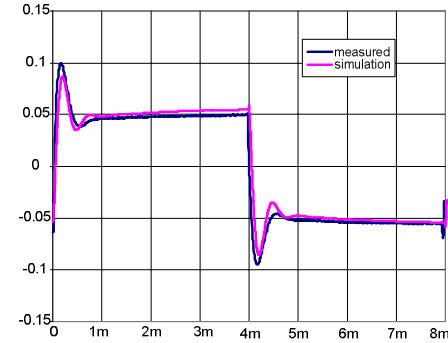


Figure 23. Measured and simulated step response of a Boost converter operated in closed loop

This study shows, however, that when the zero is near the crossover frequency, the closed-loop response will include a zero which will also increase the overshoot. The overshoot in this case can be calculated from (34).

The effect of the low loopgain at frequencies below the crossover frequencies was also analyzed. It was found that the gain has a substantial effect on the time domain closed loop response. In such cases, there is a need to take into account the effect of low frequency components of the loopgain, even though the cross over frequency set to be above ω_{pn} . As the gain decreases, one might end up with poor transient response due to the effect of these low frequency components.

ACKNOWLEDGMENT

This research was supported by the Paul Ivanier Center for Robotics and Production management.

REFERENCES

- [1] G. F. Franklin, J. D. Powell, A. Emami-Naeini, *Feedback Control of Dynamic Systems*, 5th ed, Upper Saddle River, NJ: Pearson Prentice Hall, 2006.
- [2] B. C. Kuo, *Automatic Control Systems*, 7th ed., Englewood Cliffs, NJ, Prentice Hall, 1995.
- [3] R. W. Erickson and D. Maksimovic, *Fundamentals of Power Electronics*, 2nd ed., Norwell, MA: Kluwer, 2000.
- [4] S. Ben-Yaakov, "A unified approach to teaching feedback in electronic circuit courses", *IEEE Trans. on Education*, Vol. 34, 310-316, 1991.
- [5] B. J. Patella, A. Prodic, A. Zirger, and D. Maksimovic, "High-frequency digital PWM controller IC for DC-DC converters", *IEEE Trans on PE*, Vol. 18, 1, 2,438 – 446, 2003.
- [6] Kaiwei Yao, Yu Meng, and F. C. Lee, "Control bandwidth and transient response of buck converters", *IEEE Power Electronics Specialists Conference, PESC-02 Vol. 1*, 137 – 142, Cairns, 2002.
- [7] V. Yousefzadeh, W. Narisi, Z. Popovic, and D. Maksimovic, "A digitally controlled DC/DC converter for an RF power amplifier", *IEEE Trans. on PE*, Vol. 21, 1, 164-172, 2006.
- [8] A. V. Peterchev and S. R. Sanders, "Load-Line Regulation With Estimated Load-Current Feedforward: Application to Microprocessor Voltage Regulators", *IEEE Trans on PE*, Vol 21, 6, 1704 – 1717, 2006.